Data report: major and trace element and Sr-Nd-Pb isotope analyses for basement rocks from the CRISP-A transect drilled during Expeditions 334 and 344[1]

Quanshu Yan[2, 3] and Xuefa Shi[2, 3]

Chapter contents

[1]Yan, Q., and Shi, X., 2016. Data report: major and trace element and Sr-Nd-Pb isotope analyses for basement rocks from the CRISP-A transect drilled during Expeditions 334 and 344. *In* Harris, R.N., Sakaguchi, A., Petronotis, K., and the Expedition 344 Scientists, *Proceedings of the Integrated Ocean Drilling Program,* 344: College Station, TX (Integrated Ocean Drilling Program). doi:10.2204/iodp.proc.344.205.2016
[2]Key Laboratory of Marine Sedimentary and Environmental Geology, The First Institute of Oceanography, State Oceanic Administration, Qingdao 266061, China.
Correspondence author: **yanquanshu@163.com**
[3]Also at: Laboratory for Marine Geology, Qingdao National Laboratory for Marine Science and Technology, Qingdao 266061, China.

Abstract

We report major and trace element and Sr-Nd-Pb isotope compositions of basement rocks recovered during Integrated Ocean Drilling Program (IODP) Expeditions 334 and 344 (Costa Rica Seismogenesis Project [CRISP]). The major element oxide SiO_2 was analyzed by X-ray fluorescence; all other major and trace element concentrations were determined by inductively coupled plasma–optical emission spectrometry and inductively coupled plasma–mass spectrometry, respectively. Sr, Nd, and Pb isotope ratios were analyzed by multicollector inductively coupled plasma–mass spectrometry. SiO_2 was measured at the Number 4 Exploration Institute of Geology and Mineral Resources of Shandong Province (China), and all other analytical work was carried out at Key Laboratory of Marine Sedimentary and Environmental Geology, State Oceanic Administration (China). The analyzed samples are all tholeiitic basalts that are enriched in light rare earth elements with no Eu anomalies. Most basement samples from Expedition 334 Site U1381 and Expedition 344 Site U1414 resemble enriched mid-ocean-ridge basalt. In addition, a few Hole U1414A basement samples show a positive Pb anomaly. Radiogenic isotopic (Sr, Nd, and Pb) compositions are similar to previous studies, reflecting the complexity of mantle sources and tectonic evolution of the Cocos Ridge. The trace element and Sr-Nd-Pb isotopic compositions for the recovered rocks may be further used to explain the relationship between subduction input and arc output in the subduction factory, such as the nature and role of subducted components, element cycling during subduction processing, and mantle geochemistry.

Introduction

The objective of the Costa Rica Seismogenesis Project (CRISP) was to understand the processes that control fault zone behavior during earthquake nucleation and rupture propagation in an erosional subduction zone (see the **"Expedition 344 summary"** chapter [Harris et al., 2013a]; Expedition 334 Scientists, 2012a). To achieve a comprehensive seismogenesis study, a transect was drilled from the incoming plate to the overriding plate in a single subduction system. The CRISP drilling sites are located offshore west of the Costa Rica convergent margin, which was previously identified as a site of subduction erosion (see the **"Expedition**

doi:10.2204/iodp.proc.344.205.2016

344 summary" chapter [Harris et al., 2013a]; Vannucchi et al., 2004) (Fig. F1). This area is characterized by a low sediment supply, fast convergence rate, abundant plate interface seismicity, and changing subducting plate relief along strike (see the "Expedition 344 summary" chapter [Harris et al., 2013a]; Expedition 334 Scientists, 2012a). The incoming plate is regarded as vital to seismogenesis at this location because of the variability of the subducted components (materials derived from the subducting Cocos Ridge). During the first phase of CRISP drilling (Integrated Ocean Drilling Program [IODP] Expedition 334), basement rocks were recovered from Hole U1381A. During the second phase of CRISP (IODP Expedition 344), basement rocks were recovered from both Holes U1381C and U1414A. Here we report major and trace element and Sr-Nd-Pb isotope compositions for basement rocks collected from the two sites (U1381 and U1414) drilled on the incoming plate during Expeditions 334 and 344 (Fig. F1).

Materials and methods

Study sites

Detailed descriptions of the drilling results are given in Expedition 334 Scientists (2012a, 2012b) and the "Expedition 344 summary," "Methods," and "Input Site U1414" chapters [Harris et al., 2013a, 2013b, 2013c]). Site U1381, located on the incoming plate 50 km offshore Osa Peninsula and 43 km from Caño Island (Fig. F1B), was drilled to investigate the lithostratigraphy of the sedimentary sequence on top of the Cocos Ridge as well as the uppermost portions of the ridge (Expedition 334 Scientists, 2012a). Hole U1381A sediment (90.8 m thick) was divided into two lithostratigraphic units (Expedition 334 Scientists, 2012b; Fig. F1C) and overlies >69.6 m of pillow basalt. Hole U1381C sediment (100.55 m thick) was divided into four lithostratigraphic units (see the "Methods" chapter [Harris et al., 2013b]; Fig. F1D) and overlies 0.33 m of basaltic breccia. Site U1414, located ~1 km seaward of the deformation front offshore the Osa Peninsula (Fig. F1B), was drilled to investigate the lithostratigraphy and pore water of the sedimentary sequence on top of the oceanic basement and in the uppermost portions of the underlying igneous basement (see the "Input Site U1414" chapter [Harris et al., 2013c]). Hole U1414A sediment (375.25 m thick) was divided into three units and overlies 96.35 m of oceanic basement (Fig. F1E).

Analytical methods

Sample preparation

The igneous rocks recovered from Hole U1381A mainly consist of aphyric to highly plagioclase (and/or pyroxene) phyric basalt. Vesicles are commonly filled with authigenic minerals (Expedition 334 Scientists, 2012a, 2012b), reflecting certain extents of alteration. The basement rocks recovered from Hole U1381C are brecciated basaltic fragments consisting of sparsely to highly plagioclase-clinopyroxene phenocrysts, groundmass, and vesicles (3%). Overall alteration of the basaltic groundmass is slight to moderate (see the "Expedition 344 summary" and "Methods" chapters [Harris et al., 2013a, 2013b]). The basement rocks recovered from Hole U1414A are basaltic rocks consisting of sparsely to highly plagioclase and/or pyroxene phenocrysts, groundmass, and vesicles. Alteration is slight to moderate, mainly manifested in the partial replacement of groundmass by clay minerals such as smectite (see the "Expedition 344 summary" and "Input Site U1414" chapters [Harris et al., 2013a, 2013c]).

Samples were crushed into centimeter-sized chips with a hydraulic press. The freshest fragments of each sample were then picked under a binocular microscope. These fragments were leached in 4 N nitric acid for 2 h to remove surface contamination, crushed into 0.5–1 cm^3 chips in a stainless steel mortar and pestle, rinsed in distilled water, and dried. The fragments were powdered in an alumina ceramic mill. Details of the sample preparation are the same as those described by Janney and Castillo (1996). The powdered samples were analyzed for major element, trace element, and Sr-Nd-Pb isotopic compositions.

Major and trace element analysis

The SiO_2 contents of the samples were analyzed by X-ray fluorescence (XRF) at the Number 4 Exploration Institute of Geology and Mineral Resources of Shandong Province (China). The other major element oxides and certain trace elements (Ba, Cu, Sr, V, Zn, and Cr) were determined by inductively coupled plasma–optical emission spectrometry (ICP-OES) at Key Laboratory of Marine Sedimentary and Environmental Geology, State Oceanic Administration (KLMSEG-SOA) (China). Concentrations of trace elements including high field strength elements (HFSE) (except for Zr), rare earth elements (REE), and other trace elements (i.e., Li, Be, Cr, Co, Ni, Ga, Rb, Mo, Cd, In, Cs, W, Tl, Bi, Sc, U, Th, and Pb) were measured by inductively coupled plasma–mass spectrometer (ICP-MS), also at KLMSEG-SOA. Samples were prepared by digesting 50 mg of powder with a $HF:HNO_3$ (2:1) mixture following the method described in Janney and Castillo (1996) with some modifications. Prior to ICP-OES analysis, the glass chips were ultrasonically washed twice in deionized water for 30 min and hand-picked under a binocular

microscope. The selected chips were further ultrasonically washed in quartz-distilled water. For each sample, about 25 mg of clean glass chips was digested in an ultrapure 2:1 concentrated HF:HNO_3 solution in a Teflon beaker, and then the mixture was placed on a hot plate (~60°C) and dried under a heat lamp. About 2 mL of ultrapure 12 M HNO_3 was twice added to the digested sample and evaporated to dryness. After dryness, the digested sample was diluted 4000-fold with a 2% HNO_3 solution containing 1 ppb indium as an internal standard. Precisions are ±0.2%–2% for major elements at concentrations >1 wt% (SiO_2, Al_2O_3, and CaO) and about ±2%–5% for minor elements at concentrations <1.0 wt% (MnO, K_2O, TiO_2, and P_2O_5). Loss on ignition (LOI) was also measured. The precision of this method for trace elements is within 10%. The measured values for basement rocks from Holes U1381A, U1381C, and U1414A are presented in Tables **T1** and **T2.** Accuracy was checked by measuring the United States Geological Survey chemical reference standard BHVO-2 with every batch of unknowns. The measured and recommended values for BHVO-2 for the present study are also presented in Tables **T1** and **T2.**

Sr-Nd-Pb isotopic analysis

Sr and Nd isotopic analyses were carried out for three samples from Hole U1381A, one sample from Hole U1381C, and nine samples from Hole U1414A. Pb isotopic analysis was carried out for two samples from Hole U1381A, one sample from Hole U1381C, and eight samples from Hole U1414A. Prior to dissolution, rock powders to be analyzed for Sr isotopic ratios were subjected to a harsh multistep HCl-leaching procedure (e.g., Castillo et al., 1991) to mitigate the effects of seawater alteration on $^{87}Sr/^{86}Sr$ ratios. The Sr and Nd separation procedure is similar to that described by Janney and Castillo (1996). Powders were rinsed with 0.75 M HCl for about 10 min to remove possible contamination by seawater. REEs and Sr were separated on cation ion exchange resin using HCl as the eluent, and Nd was separated from other REEs using MCI GEL CK08P cation exchange resin in alpha hydroxyisobutyric acid (α-HIBA) medium. For Pb isotopic analysis, chips of the fresh basaltic breccias were leached in ultrapure warm 6 M nitric acid for 6 h in an ultrasonic bath to remove possible Pb contamination. The samples were then rinsed with quartz-distilled water, dried, and crushed in a tungsten carbide shatterbox. About 300–400 mg of powder was digested in ultrapure 2:1 concentrated HF:HNO_3 solution in a Teflon beaker and dissolved in 1 M HBr. Lead was separated using a standard anion exchange method in a HBr medium (Lugmair and Galer, 1992). Sr, Nd, and Pb isotopic ratios were measured on a high-resolution multicollector inductively coupled plasma–mass spectrometer at KLM-SEG-SOA. $^{143}Nd/^{144}Nd$ ratios were normalized to $^{146}Nd/^{144}Nd = 0.7219$ and $^{87}Sr/^{86}Sr$ ratios to $^{86}Sr/^{88}Sr = 0.1194$. During the analysis period, the National Bureau of Standards reference material (NBS 987) yielded an average value of $^{87}Sr/^{86}Sr = 0.710268 \pm 12$ (2σ) and the JNdi-1 standard gave an average value of $^{143}Nd/^{144}Nd = 0.512120 \pm 8$ (2σ). Procedural blanks were <200 pg for Sr and <50 pg for Nd. Pb standard NBS 981 was used to correct the measured isotopic ratios of samples for isotopic fractionation; the average correction is 0.1% per atomic mass unit. During the analysis, the NBS 981 standard yielded an average value of $^{206}Pb/^{204}Pb = 16.9377$, $^{207}Pb/^{204}Pb = 15.4932$, and $^{208}Pb/^{204}Pb = 36.7247$. Initial Pb isotopic ratios were calculated from measured ratios in unleached samples using the U, Th, and Pb concentrations of the samples.

Results and discussion

Major and trace element composition and Sr-Nd-Pb isotopic ratios are reported in Tables **T1, T2,** and **T3** and are shown in Figures **F2, F3, F4, F5,** and **F6.**

Site U1381

LOI for basement samples from Site U1381 ranges from 1.55 to 4.72 wt% with an average value of 2.97 wt% (Table **T1**). These LOI values show that these rocks have suffered from seafloor weathering. This is consistent with petrographic characteristics (i.e., such as the presence of secondary hydrous/alteration minerals—clay minerals such as smectite—in the samples; see the **"Expedition 344 summary"** and **"Methods"** chapters [Harris et al., 2013a, 2013b]); Expedition 334 Scientists, 2012a). SiO_2 abundances range from 49.0 to 53.5 wt% (Table **T1**). In the total alkalis [$Na_2O + K_2O$] versus SiO_2 (TAS) diagram (Fig. **F2**), all samples from this site are basaltic and plot within the field of subalkalic (tholeiitic) rock series. All samples show high light REE to heavy REE ratios (LREE/HREE), with $(La/Yb)_N$(normalized to chondrite) = 2.2–3.1 (Table **T2**), similar to typical enriched mid-ocean-ridge basalt (E-MORB) (Sun and McDonough, 1989). There is no Eu anomaly in these rocks (Fig. **F3A**). Almost all samples show relative depletions of Ba, K, Pb, Sr, and Y. Some other large ion lithophile (LILE) and HFSE elements are slightly enriched (two times for some samples) (Fig. **F3B**), as is typical for E-MORB (Sun and McDonough, 1989). Isotopically, the Site U1381 samples show more enriched characteristics (with $^{87}Sr/^{86}Sr(i)$ ratios of 0.70357–0.70406 and $^{143}Nd/^{144}Nd(i)$ ratios of

0.51290–0.51298 (Table T3) than those from the Galapagos Islands and hotspot track (Hoernle et al., 2004) and plot between the field of depleted MORB mantle (DMM) or East Pacific Rise (EPR)/Galapagos spreading center (GSC) crust (Hoernle et al., 2000; Janney and Castillo, 1996) and enriched mantle-2 (EM2) (Zindler and Hart, 1986) (Fig. F5). All Pb isotope data show slight variations ($^{206}Pb/^{204}Pb(t)$ = 18.770–18.993, $^{207}Pb/^{204}Pb(t)$ = 15.586–15.602, and $^{208}Pb/^{204}Pb(t)$ = 38.621–38.761) (Table T3) and basically plot between EPR/GSC crust and Cocos Ridge (Hoernle et al., 2004, 2008; Gazel et al., 2009) (Fig. F6). Because the samples have been carefully leached, the isotopic compositions provided above may basically represent the actual compositions.

Hole U1414A

LOI values of basaltic basement samples from Hole U1414A show large variations, ranging from 0.54 to 6.73 wt% with an average value of 2.26 wt% (Table T1). This variation shows that most samples suffered seafloor weathering. This is consistent with petrographic characteristics, such as the presence of secondary hydrous/alteration minerals (e.g., smectite) in the samples (see the **"Expedition 344 summary"** and **"Input Site U1414"** chapters [Harris et al., 2013a, 2013c]). In addition to one sample (344-U1414A-56R-2W, 22–28 cm) with a higher SiO_2 of 57.4 wt% (Fig. F2), the contents of SiO_2 for all other Hole U1414A samples range from 48.5 to 54.4 wt% (Table T1). In the TAS diagram (Fig. F2), similar to the case for Site U1381 samples, all Hole U1414A samples are basaltic and plot within the field of subalkalic (tholeiitic) rock series. All samples from this hole show high LREE/HREE ratios, with $(La/Yb)_N$(normalized to chondrite) = 1.9–4.1 (Table T2), similar to E-MORB (Sun and McDonough, 1989). There is no Eu anomaly (Fig. F4A). A few samples are slightly enriched in K, Pb, and Sr, and almost all samples generally show relative depletions of Ba, K, Pb, Sr, and Y and slight enrichment of some incompatible elements (e.g., Nb, Ta, La, and Ce) (Fig. F4B). Again, this is typical for E-MORB (Sun and McDonough, 1989). Isotopically, the Hole U1414A samples are more inhomogeneous (with $^{87}Sr/^{86}Sr(i)$ ratios of 0.70275–0.70406 and $^{143}Nd/^{144}Nd(i)$ ratios of 0.51278–0.51302) (Table T3) than those from Site U1381. In addition to one sample (344-U1414A-51R-4W, 126–134 cm) plotting close to EPR/GSC crust, all other samples plot between the field of DMM or EPR/GSC crust and EM2 (Fig. F5). All Pb isotope data ($^{206}Pb/^{204}Pb(t)$ = 18.424–19.283, $^{207}Pb/^{204}Pb(t)$ = 15.570–15.609, and $^{208}Pb/^{204}Pb(t)$ = 38.360–38.911) (Table T3) show more variability than those from Site U1381 (Fig. F6). Isotopic compositions indicate mantle heterogeneity below the Cocos Ridge (at least for the drilled part of the ridge). A new petrogenetic model will be necessary for interpreting the observable differences in isotopic compositions between the present work and previous studies for other parts of the Cocos Ridge.

Acknowledgments

This research used samples and data provided by the International Ocean Discovery Program (IODP). The outstanding efforts of the Siem Offshore officers and crew as well as the drilling personnel and the scientific parties of IODP Expeditions 334 and 344 are greatly acknowledged here. We thank anonymous reviewers for reviewing this manuscript and Katerina Petronotis for editorial handling and helpful comments. This study was supported by National Natural Science Foundation of China (NSFC numbers 41322036, 41276003 and 41296030) and IODP-China.

References

Castillo, P.R., Carlson, R.W., and Batiza, R., 1991. Origin of Nauru Basin igneous complex: Sr, Nd, and Pb isotope and REE constraints. *Earth and Planetary Science Letters,* 103(1–4):200–213. **http://dx.doi.org/10.1016/0012-821X(91)90161-A**

Expedition 334 Scientists, 2012a. Expedition 334 summary. *In* Vannucchi, P., Ujiie, K., Stroncik, N., Malinverno, A., and the Expedition 334 Scientists, *Proceedings of the Integrated Ocean Drilling Program,* 334: Tokyo (Integrated Ocean Drilling Program Management International, Inc.). **http://dx.doi.org/10.2204/iodp.proc.334.101.2012**

Expedition 334 Scientists, 2012b. Site U1381. *In* Vannucchi, P., Ujiie, K., Stroncik, N., Malinverno, A., and the Expedition 334 Scientists, *Proceedings of the Integrated Ocean Drilling Program,* 334: Tokyo (Integrated Ocean Drilling Program Management International, Inc.). **http://dx.doi.org/10.2204/iodp.proc.334.106.2012**

Gazel, E., Carr, M.J., Hoernle, K., Feigenson, M.D., Szymanski, D., Hauff, F., and van den Bogaard, P., 2009. Galapagos-OIB signature in southern Central America: mantle refertilization by arc–hot spot interaction. *Geochemistry, Geophysics, Geosystems,* 10(2):Q02S11. **http://dx.doi.org/10.1029/2008GC002246**

Harris, R.N., Sakaguchi, A., Petronotis, K., Baxter, A.T., Berg, R., Burkett, A., Charpentier, D., Choi, J., Diz Ferreiro, P., Hamahashi, M., Hashimoto, Y., Heydolph, K., Jovane, L., Kastner, M., Kurz, W., Kutterolf, S.O., Li, Y., Malinverno, A., Martin, K.M., Millan, C., Nascimento, D.B., Saito, S., Sandoval Gutierrez, M.I., Screaton, E.J., Smith-Duque, C.E., Solomon, E.A., Straub, S.M., Tanikawa, W., Torres, M.E., Uchimura, H., Vannucchi, P.,

Yamamoto, Y., Yan, Q., and Zhao, X., 2013a. Expedition 344 summary. *In* Harris, R.N., Sakaguchi, A., Petronotis, K., and the Expedition 344 Scientists, *Proceedings of the Integrated Ocean Drilling Program,* 344: College Station, TX (Integrated Ocean Drilling Program). **http://dx.doi.org/10.2204/iodp.proc.344.101.2013**

Harris, R.N., Sakaguchi, A., Petronotis, K., Baxter, A.T., Berg, R., Burkett, A., Charpentier, D., Choi, J., Diz Ferreiro, P., Hamahashi, M., Hashimoto, Y., Heydolph, K., Jovane, L., Kastner, M., Kurz, W., Kutterolf, S.O., Li, Y., Malinverno, A., Martin, K.M., Millan, C., Nascimento, D.B., Saito, S., Sandoval Gutierrez, M.I., Screaton, E.J., Smith-Duque, C.E., Solomon, E.A., Straub, S.M., Tanikawa, W., Torres, M.E., Uchimura, H., Vannucchi, P., Yamamoto, Y., Yan, Q., and Zhao, X., 2013b. Input Site U1381. *In* Harris, R.N., Sakaguchi, A., Petronotis, K., and the Expedition 344 Scientists, *Proceedings of the Integrated Ocean Drilling Program,* 344: College Station, TX (Integrated Ocean Drilling Program). **http://dx.doi.org/10.2204/iodp.proc.344.103.2013**

Harris, R.N., Sakaguchi, A., Petronotis, K., Baxter, A.T., Berg, R., Burkett, A., Charpentier, D., Choi, J., Diz Ferreiro, P., Hamahashi, M., Hashimoto, Y., Heydolph, K., Jovane, L., Kastner, M., Kurz, W., Kutterolf, S.O., Li, Y., Malinverno, A., Martin, K.M., Millan, C., Nascimento, D.B., Saito, S., Sandoval Gutierrez, M.I., Screaton, E.J., Smith-Duque, C.E., Solomon, E.A., Straub, S.M., Tanikawa, W., Torres, M.E., Uchimura, H., Vannucchi, P., Yamamoto, Y., Yan, Q., and Zhao, X., 2013c. Input Site U1414. *In* Harris, R.N., Sakaguchi, A., Petronotis, K., and the Expedition 344 Scientists, *Proceedings of the Integrated Ocean Drilling Program,* 344: College Station, TX (Integrated Ocean Drilling Program). **http://dx.doi.org/10.2204/iodp.proc.344.104.2013**

Hart, S.R., 1984. A large-scale isotope anomaly in the Southern Hemisphere mantle. *Nature,* 309(5971):753–757. **http://dx.doi.org/10.1038/309753a0**

Hoernle, K., Abt, D.L., Fischer, K.M., Nichols, H., Hauff, F., Abers, G.A., van den Bogaard, P., Heydolph, K., Alvarado, G., Protti, M., and Strauch, W., 2008. Arc-parallel flow in the mantle wedge beneath Costa Rica and Nicaragua. *Nature,* 451(7182):1094–1097. **http://dx.doi.org/10.1038/nature06550**

Hoernle, K., Hauff, F., and van den Bogaard, P., 2004. 70 m.y. history (139–69 Ma) for the Caribbean large igneous province. *Geology,* 32(8):697–700. **http://dx.doi.org/10.1130/G20574.1**

Hoernle, K., Werner, R., Phipps Morgan, J., Garbe-Schönberg, D., Bryce, J., and Mrazek, J., 2000. Existence of complex spatial zonation in the Galápagos plume. *Geology,* 28(5):435–438. **http://dx.doi.org/10.1130/0091-7613(2000)028<0435:EOCSZI>2.3.CO;2**

Irvine, T.N., and Baragar, W.R.A., 1971. A guide to the chemical classification of the common volcanic rocks. *Canadian Journal of Earth Sciences,* 8(5):523–548. **http://dx.doi.org/10.1139/e71-055**

Janney, P.E., and Castillo, P.R., 1996. Basalts from the Central Pacific Basin: evidence for the origin of Cretaceous igneous complexes in the Jurassic western Pacific. *Journal of Geophysical Research: Solid Earth,* 101(B2):2875–2893. **http://dx.doi.org/10.1029/95JB03119**

Le Maitre, R.W., 1989. *A Classification of Igneous Rocks and Glossary of Terms:* Oxford, UK (Blackwell Sci. Publ.).

Lugmair, G.W., and Galer, S.J.G., 1992. Age and isotopic relationships among the angrites Lewis Cliff 86010 and Angra dos Reis. *Geochimica et Cosmochimica Acta,* 56(4):1673–1694. **http://dx.doi.org/10.1016/0016-7037(92)90234-A**

Niu, Y., and O'Hara, M.J., 2003. Origin of ocean island basalts: a new perspective from petrology, geochemistry, and mineral physics considerations. *Journal of Geophysical Research: Solid Earth,* 108(B4):2209. **http://dx.doi.org/10.1029/2002JB002048**

Sun, S.-S., and McDonough, W.F., 1989. Chemical and isotopic systematics of oceanic basalts: implications for mantle composition and processes. *In* Saunders, A.D., and Norry, M.J. (Eds.), *Magmatism in the Ocean Basins.* Geological Society Special Publication, 42(1):313–345. **http://dx.doi.org/10.1144/GSL.SP.1989.042.01.19**

Vannucchi, P., Galeotti, S., Clift, P.D., Ranero, C.R., and von Huene, R., 2004. Long-term subduction-erosion along the Guatemalan margin of the Middle America Trench. *Geology*, 32(7):617–620. **http://dx.doi.org/10.1130/G20422.1**

Zindler, A., and Hart, S., 1986. Chemical geodynamics. *Annu. Rev. Earth Planet. Sci.,* 14:493–571. **http://dx.doi.org/10.1146/annurev.ea.14.050186.002425**

Initial receipt: 12 August 2015
Acceptance: 21 December 2015
Publication: 19 February 2016
MS 344-205

Figure F1. A. Geological map and locations of sites drilled during IODP Costa Rica Seismogenesis Project (CRISP). EPR = East Pacific Rise. **B.** Location of Sites U1381 and U1414 drilled during Expeditions 334 and 344. A new hole was drilled at Site U1381 during Expedition 344. **C.** Lithostratigraphic units for Hole U1381A (from Expedition 334 Scientists, 2012a). **D, E.** Lithostratigraphic units for Holes 1381C and U1414A (from the "Expedition 344 summary" chapter [Harris et al., 2013a]).

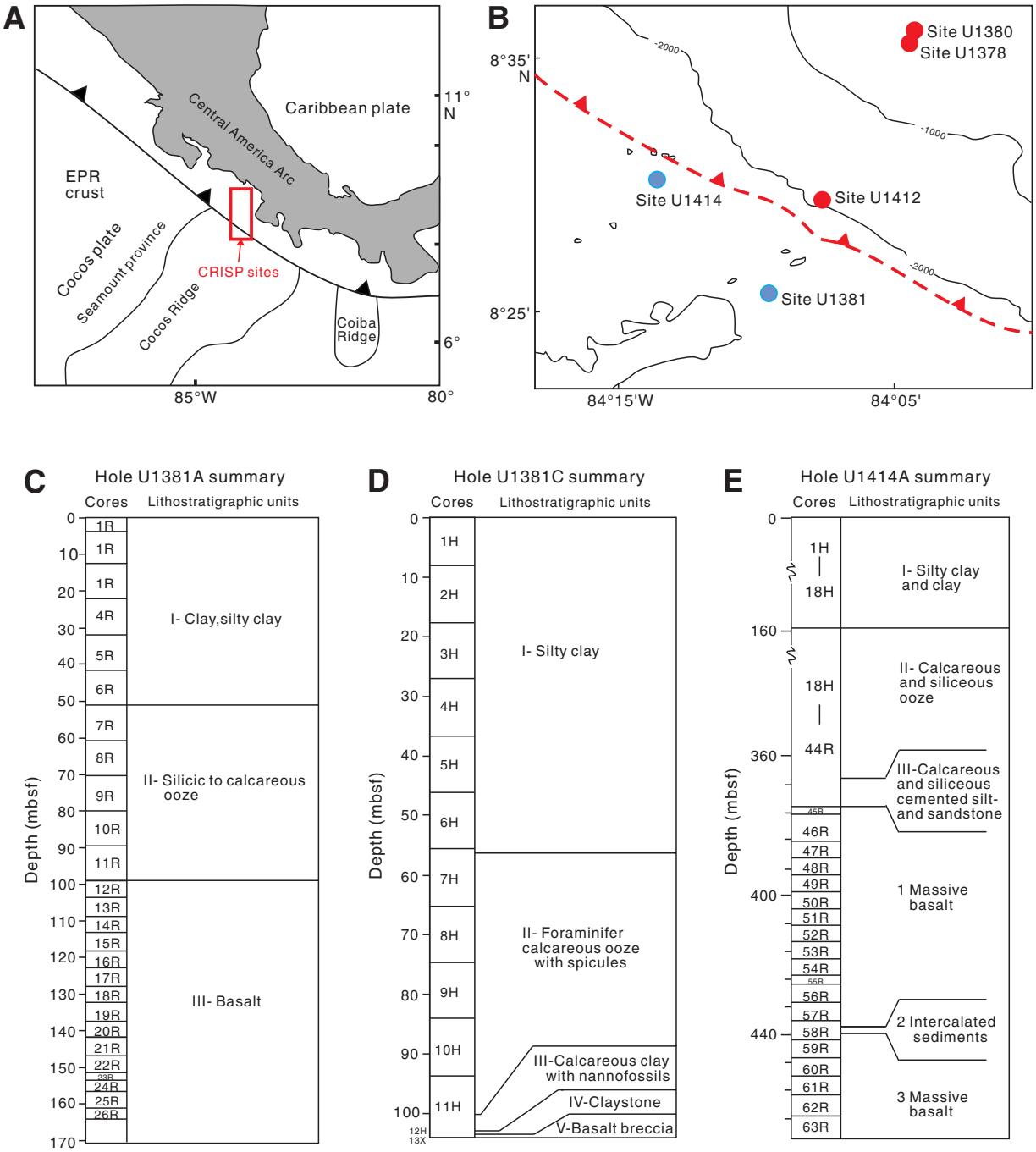

Figure F2. Total alkalis vs. silica ($Na_2O + K_2O$ vs. SiO_2) and alkaline discrimination diagrams for basement rocks from the CRISP-A transect drilled during Expeditions 334 and 344 (Le Maitre, 1989). The line dividing alkalic and tholeiitic series is from Irvine and Baragar (1971). The fields for north, central, and south Cocos Ridge (including seamounts in the north) are from Hoernle et al. (2000).

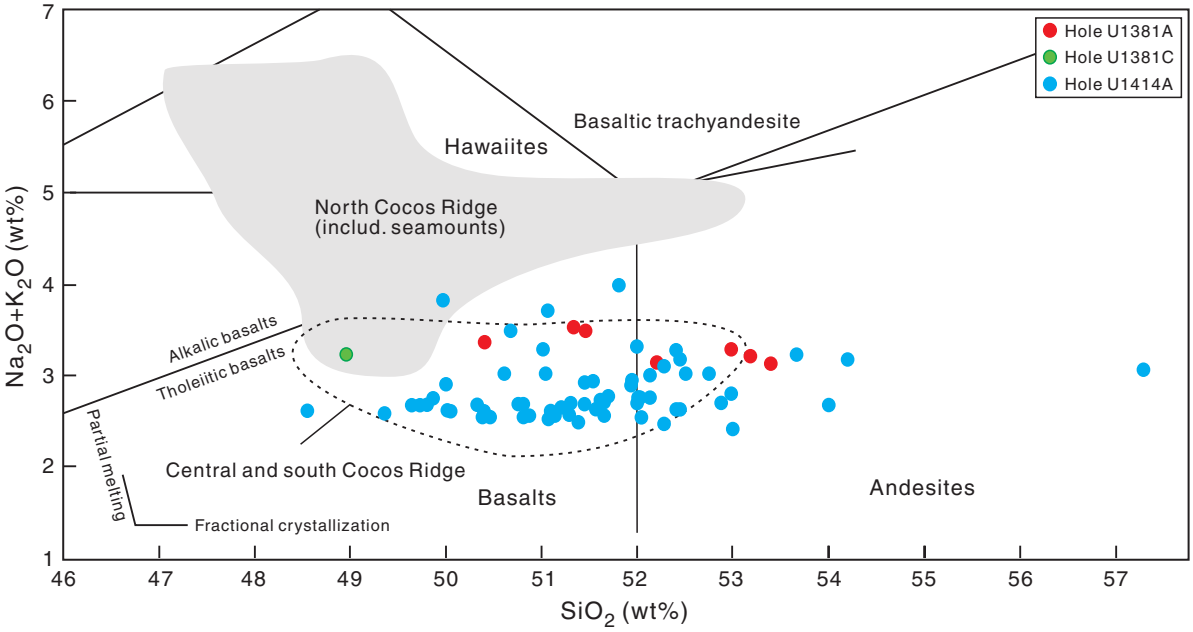

Figure F3. (**A**) Primitive mantle-normalized trace element concentration diagrams and (**B**) C1 chondrite-normalized REE abundance patterns for basement rocks from Site U1381 (Holes U1381A and U1381C). Data for primitive mantle and C1 chondrite are from Sun and McDonough (1989). Data for normal mid-ocean-ridge basalt (N-MORB), enriched mid-ocean-ridge basalt (E-MORB), and ocean island basalt (OIB) are from Niu and O'Hara (2003).

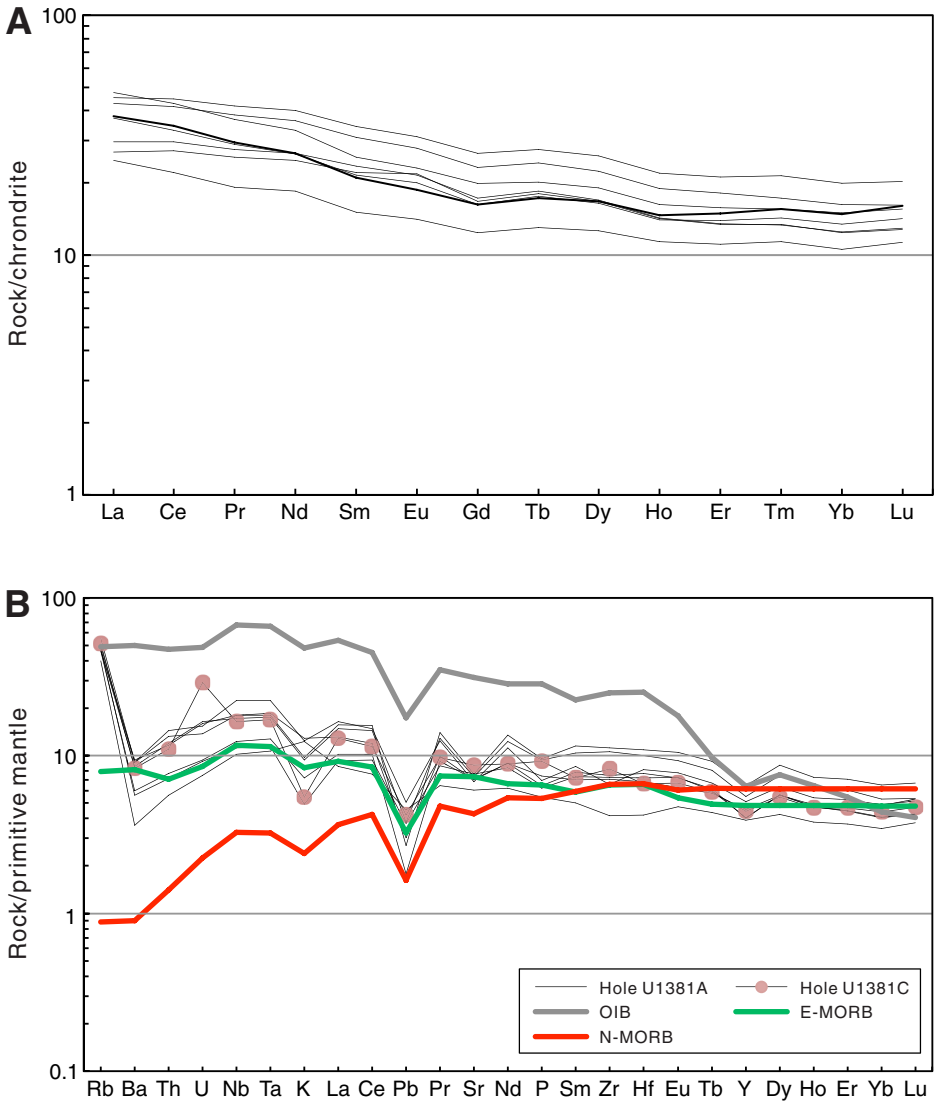

Figure F4. (**A**) Primitive mantle-normalized trace element concentration diagrams and (**B**) C1 chondrite-normalized REE abundances patterns for basement rocks from Site U1414 (Hole U1414A). Data for primitive mantle and C1 chondrite are from Sun and McDonough (1989). Data for normal mid-ocean-ridge basalt (N-MORB), enriched mid-ocean-ridge basalt (E-MORB), and ocean island basalt (OIB) are from Niu and O'Hara (2003).

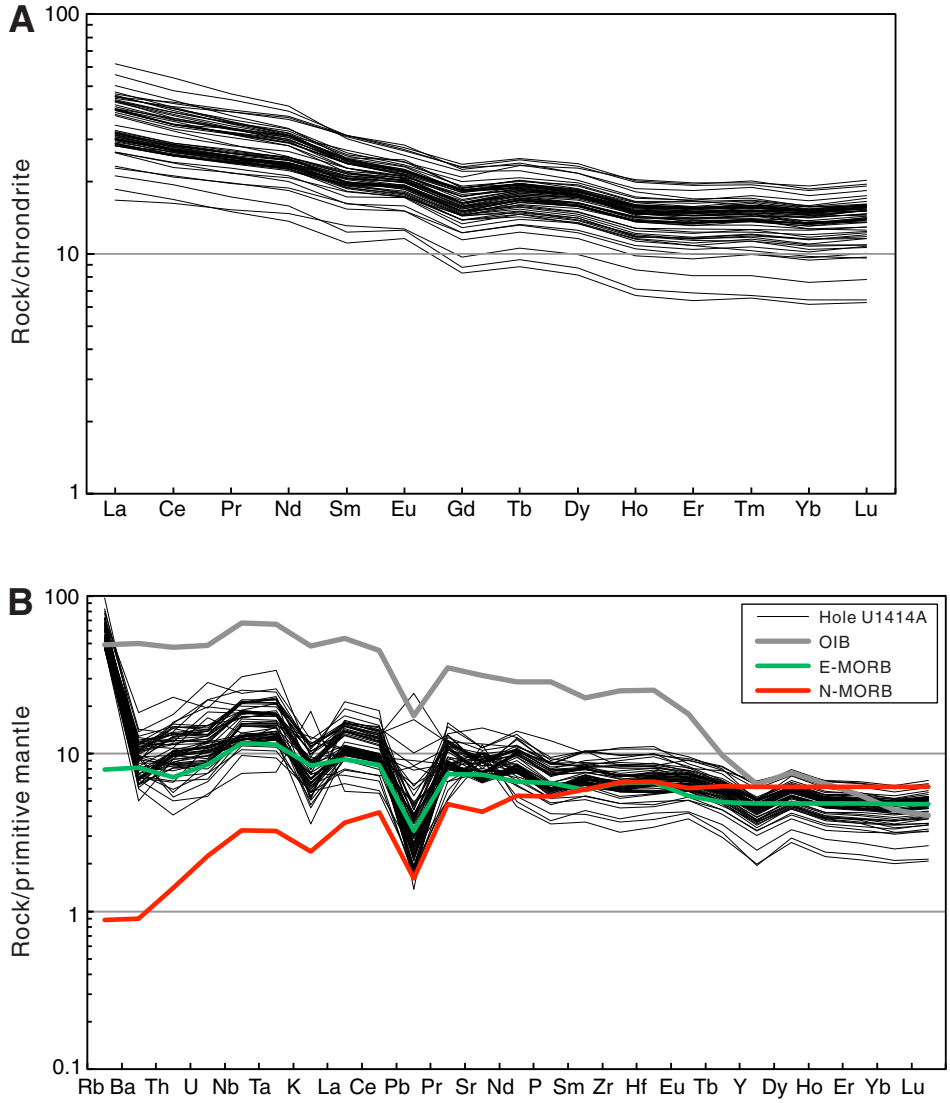

Figure F5. $^{143}Nd/^{144}Nd(i)$ vs. $^{87}Sr/^{86}Sr(i)$ diagram for basement rocks from the CRISP-A transect drilled during Expeditions 334 and 344. Approximate fields for the proposed depleted mantle MORB (DMM), high μ (HIMU), enriched mantle 1 (EM1) and 2 (EM2) mantle end-members are from Zindler and Hart (1986). The shaded field for East Pacific Rise (EPR)/Galapagos spreading center (GSC) crust is from Hoernle et al. (2000) and Janney and Castillo (1996). The pink field for Galapagos Islands and hotspot track is from Hoernle et al. (2004).

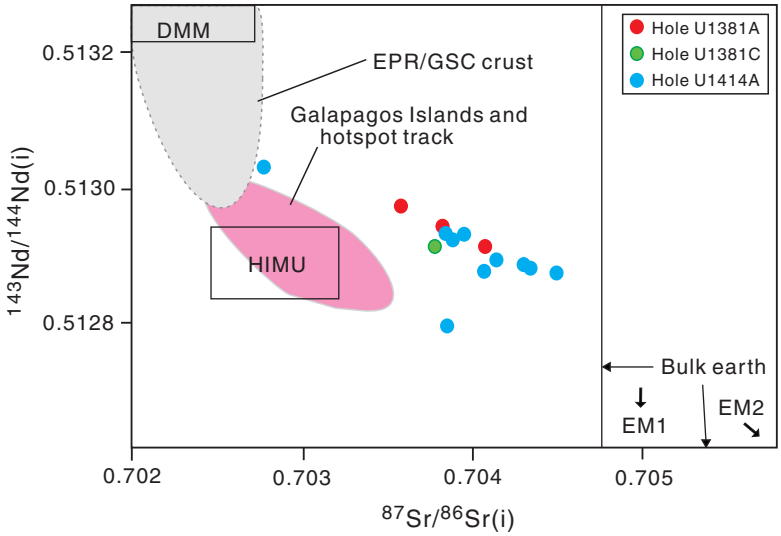

Figure F6. (**A**) $^{208}Pb/^{206}Pb(t)$ vs. $^{206}Pb/^{204}Pb(t)$ and (**B**) $^{143}Nd/^{144}Nd(i)$ vs. $^{206}Pb/^{204}Pb(t)$ diagrams for basement rocks from the CRISP-A transect drilled during Expeditions 334 and 344. The shaded field for East Pacific Rise (EPR)/Galapagos spreading center (GSC) crust is the same as in Figure F5. The pink field for Cocos Ridge is from Hoernle et al. (2004, 2008) and Gazel et al. (2009). The Northern Hemisphere reference line (NHRL) is from Hart (1984).

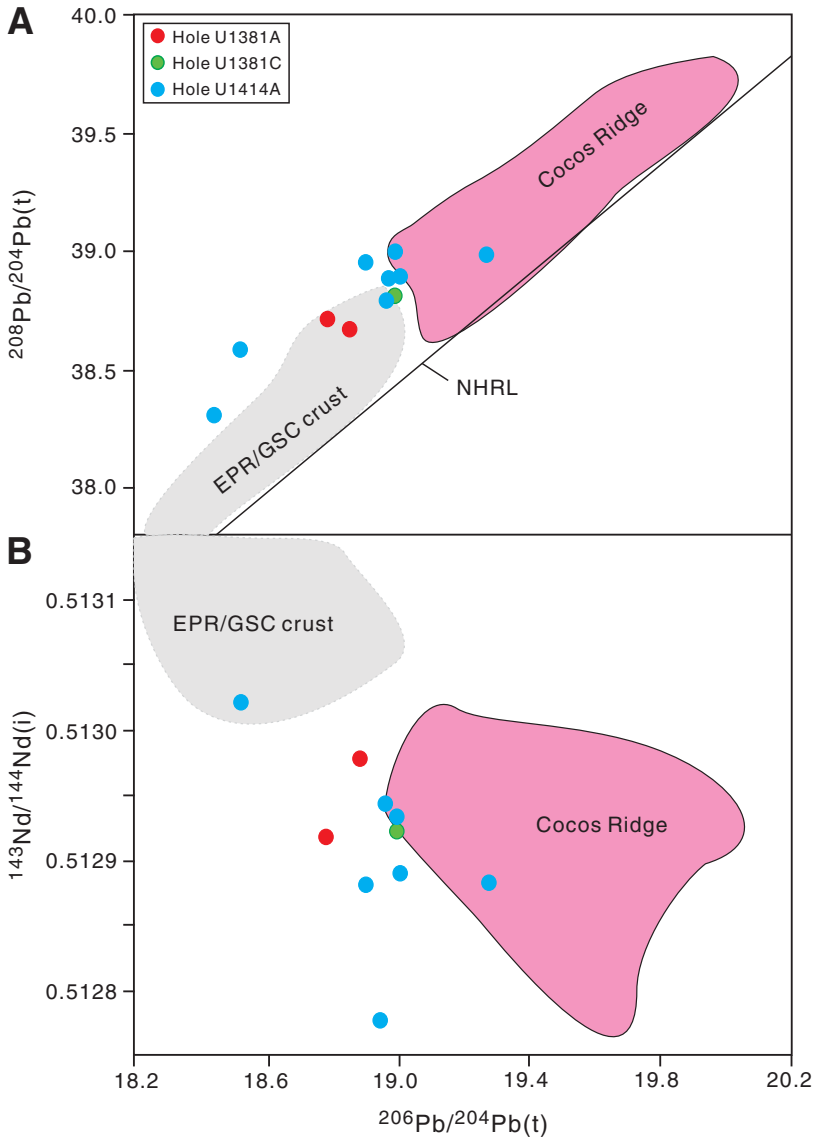

Table T1. Major element compositions in basement rocks from Sites U1381 and U1414, Expeditions 334 and 344. (Continued on next page.)

Core, section, interval (cm)	SiO_2 (wt%)	TiO_2 (wt%)	Al_2O_3 (wt%)	TFe_2O_3 (wt%)	MnO (wt%)	MgO (wt%)	CaO (wt%)	Na_2O (wt%)	K_2O (wt%)	P_2O_5 (wt%)	LOI (wt%)
334-U1381A-											
16R-2, 136–139	53.49	0.99	10.32	12.50	0.06	10.19	5.55	2.81	0.40	0.13	3.57
16R-2, 134–137	51.43	1.97	12.80	12.00	0.11	8.24	6.63	3.18	0.29	0.21	3.11
18R-2, 1–4	53.22	1.66	11.52	11.73	0.10	8.20	7.30	3.10	0.23	0.15	2.79
20R-2, 115–118	51.35	2.16	12.10	13.61	0.12	7.89	6.70	3.27	0.30	0.21	2.28
22R-3, 8–13	52.31	1.69	12.88	11.21	0.12	7.11	9.87	2.95	0.16	0.14	1.55
26R-1, 80–83	50.40	1.38	11.28	13.38	0.09	10.96	5.69	2.93	0.41	0.17	3.31
26R-3, 53–56	53.04	1.39	10.20	13.44	0.09	10.31	5.64	2.88	0.40	0.16	2.44
344-U1381C-											
13X-1, 11–16	48.97	1.65	13.13	12.15	0.12	7.49	8.33	3.06	0.17	0.21	4.72
344-U1414A-											
45R-1, 65–71	51.78	2.21	14.68	9.54	0.09	6.29	8.22	3.49	0.35	0.22	3.14
45R-2, 82–92	51.48	1.95	12.64	12.09	0.18	5.62	11.45	2.63	0.23	0.19	1.53
46R-1, 107–110	49.69	1.91	13.26	13.63	0.20	6.30	11.34	2.51	0.16	0.19	0.81
46R-2, 132–138	51.69	1.21	12.24	12.31	0.17	7.28	10.12	2.57	0.16	0.12	2.14
47R-1, 47–53	52.50	0.98	10.74	11.84	0.09	10.59	5.50	2.54	0.61	0.09	4.52
47R-4, 27–34	51.11	1.26	14.35	11.06	0.14	7.07	11.25	2.31	0.23	0.13	1.10
48R-1, 117–122	51.74	1.34	12.31	11.26	0.13	7.02	11.36	2.34	0.20	0.13	2.16
48R-3, 26–36	52.98	1.14	12.47	10.44	0.13	6.34	12.69	2.24	0.18	0.11	1.27
49R-2, 91–98	52.36	1.72	12.12	13.06	0.16	7.37	6.81	2.94	0.35	0.20	2.92
50R-2, 100–109	50.97	1.73	12.84	13.16	0.10	7.62	6.88	2.89	0.34	0.19	3.27
51R-1, 90–101	53.69	1.63	12.19	12.58	0.12	6.50	7.65	2.89	0.35	0.20	2.22
51R-2, 35–44	52.32	1.65	12.84	12.75	0.12	6.93	7.62	2.76	0.31	0.18	2.53
51R-4, 126–134	52.34	0.85	14.63	7.87	0.10	6.67	12.60	2.17	0.19	0.08	2.50
52R-1, 82–90	54.02	0.94	14.68	7.92	0.11	5.86	11.41	2.43	0.25	0.10	2.27
52R-1, 98–105	51.07	1.84	14.37	11.72	0.19	6.44	7.02	3.38	0.37	0.21	3.40
53R-1, 38–46	52.22	1.55	13.69	11.60	0.14	6.70	9.19	2.71	0.26	0.17	1.78
53R-4, 0–6	52.08	1.52	12.42	13.42	0.18	6.25	10.46	2.49	0.28	0.17	0.73
54R-1, 12–23	52.86	1.47	12.35	13.13	0.17	6.13	10.31	2.46	0.26	0.16	0.69
54R-1, 121–130	52.01	1.47	12.97	13.13	0.17	6.52	10.30	2.47	0.26	0.16	0.54
54R-2, 74–84	50.83	1.42	11.82	12.63	0.17	5.96	10.15	2.42	0.25	0.16	4.19
54R-3, 82–92	51.98	1.47	12.14	13.35	0.18	6.32	10.68	2.46	0.26	0.16	1.00
54R-4, 68–72	51.83	1.52	12.57	13.35	0.18	6.38	10.49	2.49	0.27	0.17	0.76
54R-5, 71–75	52.19	1.51	12.57	13.07	0.19	6.10	10.74	2.54	0.32	0.17	0.61
55R-1, 6–15	50.63	1.27	12.35	12.50	0.14	10.07	6.12	2.66	0.38	0.14	3.73
55R-1, 39–44	51.07	1.29	11.35	13.09	0.12	10.04	5.64	2.66	0.41	0.14	4.18
55R-1, 89–98	52.78	1.28	11.79	11.71	0.14	8.82	6.75	2.63	0.30	0.15	3.65
55R-2, 17–26	49.66	1.16	15.88	10.24	0.12	8.64	8.98	2.48	0.14	0.13	2.56
55R-2, 59–69	51.73	1.24	13.05	10.29	0.14	7.17	10.51	2.54	0.15	0.14	3.06
55R-3, 12–19	52.07	1.11	14.17	9.68	0.13	7.57	10.34	2.32	0.20	0.11	2.30
56R-1, 109–115	51.18	1.15	13.92	10.09	0.11	7.83	10.32	2.34	0.23	0.12	2.73
56R-2, 22–28	57.38	1.29	7.49	11.35	0.13	6.12	11.35	2.59	0.29	0.15	1.87
57R-1, 32–37	52.04	1.41	13.19	11.52	0.14	7.82	8.95	2.49	0.26	0.13	2.03
57R-1, 76–81	50.07	1.40	15.25	11.27	0.15	8.23	8.68	2.57	0.28	0.14	1.97
58R-2, 41–44	50.66	1.64	13.05	13.53	0.15	7.51	6.47	3.16	0.34	0.20	3.30
58R-3, 0–6	52.14	1.55	13.27	12.46	0.17	7.11	6.84	3.00	0.38	0.19	2.88
59R-1, 66–72	54.39	1.39	11.34	12.48	0.16	7.99	5.81	2.94	0.28	0.26	2.96
59R-2, 82–87	52.50	1.39	13.38	12.03	0.14	7.53	7.51	2.67	0.31	0.15	2.40
60R-1, 22–28	51.68	1.29	12.81	12.03	0.13	6.95	9.73	2.57	0.24	0.18	2.39
60R-1, 92–100	51.98	1.45	12.86	12.55	0.14	6.61	10.00	2.61	0.25	0.18	1.38
60R-2, 55–65	50.33	1.31	14.05	12.39	0.12	8.09	8.97	2.44	0.16	0.16	1.97
60R-3, 6–13	51.62	1.36	12.34	12.78	0.14	7.58	9.08	2.66	0.27	0.14	2.03
60R-3, 109–117	51.94	1.38	12.58	12.64	0.15	7.33	8.70	2.60	0.34	0.17	2.17
61R-1, 16–23	49.86	1.87	14.93	12.63	0.24	6.22	7.62	3.39	0.32	0.19	2.72
61R-1, 90–97	51.38	1.49	11.97	14.15	0.17	6.81	9.12	2.52	0.17	0.14	2.08
61R-1, 123–129	52.96	1.53	9.54	15.18	0.17	6.39	9.27	2.60	0.18	0.15	2.04
61R-2, 19–27	48.47	1.34	11.05	14.04	0.15	7.24	8.34	2.35	0.17	0.12	6.73
61R-2, 108–115	51.28	1.52	11.42	15.00	0.17	6.93	8.93	2.49	0.20	0.14	1.93
61R-3, 25–33	52.19	1.47	11.14	14.72	0.17	6.89	8.71	2.49	0.22	0.14	1.86
62R-1, 7–14	50.08	1.46	12.02	14.61	0.15	7.22	8.32	2.43	0.18	0.14	3.39
62R-1, 59–65	51.59	1.34	11.78	14.09	0.14	6.45	9.32	2.39	0.22	0.14	2.53
62R-2, 19–34	49.82	1.69	12.45	16.29	0.18	7.13	8.05	2.48	0.24	0.17	1.51
62R-2, 54–61	52.36	1.33	12.39	13.61	0.15	6.16	10.04	2.41	0.20	0.12	1.24
62R-2, 117–125	51.41	1.45	11.35	14.64	0.16	6.65	9.52	2.37	0.11	0.12	2.23
62R-3, 75–82	51.11	1.40	12.02	13.95	0.17	6.65	9.56	2.34	0.19	0.13	2.48
62R-4, 50–57	50.51	1.37	13.66	13.65	0.16	6.80	10.20	2.35	0.20	0.12	0.98

Table T1 (continued).

Core, section, interval (cm)	SiO_2 (wt%)	TiO_2 (wt%)	Al_2O_3 (wt%)	TFe_2O_3 (wt%)	MnO (wt%)	MgO (wt%)	CaO (wt%)	Na_2O (wt%)	K_2O (wt%)	P_2O_5 (wt%)	LOI (wt%)
62R-4, 70–78	50.41	1.36	13.72	13.54	0.16	7.26	9.61	2.36	0.20	0.12	1.27
63R-1, 25–34	50.52	1.37	12.56	14.09	0.16	6.96	9.49	2.34	0.20	0.12	2.18
63R-1, 96–104	49.40	1.34	13.26	14.10	0.16	7.52	9.26	2.31	0.21	0.13	2.31
63R-2, 25–33	51.17	1.33	12.35	13.87	0.15	7.21	9.17	2.37	0.21	0.13	2.05
63R-2, 111–118	51.67	1.41	12.29	13.82	0.13	7.28	8.42	2.47	0.21	0.13	2.17
63R-3, 50–57	51.25	1.36	12.85	13.64	0.15	7.23	9.03	2.36	0.21	0.13	1.78
63R-3, 79–88	51.16	1.41	12.79	13.91	0.14	7.60	8.54	2.40	0.20	0.13	1.72
63R-3, 100–110	50.95	1.41	12.46	14.07	0.15	7.43	8.88	2.39	0.19	0.13	1.95
63R-4, 14–27	50.77	1.36	13.13	13.60	0.16	7.05	9.32	2.35	0.21	0.13	1.91
BHVO-2 (measured)	49.87	2.71	13.6	12.28		7.25	11.5	2.22	0.53	0.26	
BHVO-2 (recommended)	49.9	2.73	13.5	12.3		7.23	11.4	2.22	0.52	0.27	

Table T2. Trace element compositions in basement rocks from Sites U1381 and U1414, Expeditions 334 and 344. This table is available in an **oversized format.**

Table T3. Strontium, Nd, and Pb isotopic ratios in basement rocks from Sites U1381 and U1414, Expeditions 334 and 344.

Core, section, interval (cm)	$^{87}Sr/^{86}Sr$	2σ	$^{87}Sr/^{86}Sr(i)$	$^{143}Nd/^{144}Nd$	2σ	$^{143}Nd/^{144}Nd(i)$	$^{206}Pb/^{204}Pb$	2σ	$^{207}Pb/^{204}Pb$	2σ	$^{208}Pb/^{204}Pb$	2σ	$^{206}Pb/^{204}Pb(t)$	$^{207}Pb/^{204}Pb(t)$	$^{208}Pb/^{204}Pb(t)$
334-U1381A-															
16R-2, 136–139	0.704189	0.000010	0.70406	0.512938	0.000015	0.512922	18.8046	0.00023	15.5900	0.00014	38.7306	0.00015	18.770	15.588	38.697
20R-2, 115–118	0.703702	0.000018	0.70357	0.512993	0.000012	0.512976	18.9502	0.00014	15.5905	0.00015	38.7542	0.00016	18.844	15.586	38.621
26R-3, 53–56	0.703951	0.000013	0.70379	0.512918	0.000013	0.512902									
344-U1381C-															
13X-1, 11–16	0.703869	0.000011	0.70375	0.512940	0.000015	0.512923	19.1378	0.00018	15.6090	0.00013	38.8320	0.00020	18.993	15.602	38.761
344-U1414A-															
46R-1, 107–110	0.704071	0.000015	0.70394	0.512951	0.000023	0.512934	18.4646	0.00025	15.6046	0.00014	38.4018	0.00029	18.424	15.603	38.360
48R-1, 117–122	0.703945	0.000015	0.70381	0.512794	0.000011	0.512776	19.0133	0.00012	15.5929	0.00013	38.8510	0.00011	18.968	15.591	38.799
51R-4, 126–134	0.702889	0.000012	0.70275	0.513040	0.000022	0.513023	18.5607	0.00014	15.5723	0.00024	38.6432	0.00011	18.514	15.570	38.586
54R-1, 12–23							19.0498	0.00025	15.5952	0.00023	38.8735	0.00019	18.951	15.591	38.743
56R-1, 109–115	0.704306	0.000014	0.70417	0.512917	0.000025	0.512900									
58R-3, 0–6	0.704632	0.000018	0.70449	0.512895	0.000016	0.512879	19.4383	0.00026	15.6164	0.00026	38.9566	0.00017	19.2827	15.609	38.829
59R-2, 82–87	0.704433	0.000018	0.70430	0.512905	0.000013	0.512889	19.0523	0.00019	15.5831	0.00014	38.9921	0.00011	18.9953	15.580	38.911
59R-2, 82–87*	0.704465	0.000022	0.70433	0.512908	0.000012	0.512893									
60R-2, 55–65	0.704229	0.000012	0.70409	0.512900	0.000015	0.512884	18.9706	0.00015	15.5887	0.00015	38.9628	0.00011	18.904	15.586	38.877
62R-2, 117–125	0.703954	0.000011	0.70382	0.512961	0.000018	0.512943	19.0417	0.00020	15.5921	0.00024	38.8624	0.00010	18.975	15.589	38.780

* = duplicate sample. Initial Sr, Nd, and Pb isotopic ratios for these samples are calculated using an age of 16 Ma (Hoernle et al., 2000).